Proceedings of the 17th World Congress
The International Federation of Automatic Control
Seoul, Korea, July 6-11, 2008

Model-based fault detection and diagnosis with special input excitation applied to a modern diesel engine ⋆

Sebastian Clever * **Rolf Isermann** *

* *Institute of Automatic Control, Technische Universität Darmstadt, Darmstadt, Germany, (e-mail: [SClever, RIsermann]@iat.tu-darmstadt.de)*

Abstract: Due to the rising complexity of many technical processes modern diagnosis systems have to supervise a multitude of hydraulic, mechanical, electromechanical and mechatronic components. Therefore model-based methods of fault-detection and diagnosis have been developed. These methods use mathematical process models to relate data of several measurable variables. Thus the diagnosis quality depends on the available sensor data. In order to obtain additional information with the given sensor configuration special input excitation signals can be used. This paper will describe a method to locate faults in multivariable systems using such input excitation and its application to the intake air system of a modern common rail Diesel engine. The presented method uses the knowledge of fault effects on the measured output, when the inputs are successively excited quasi-stationary, to determine the location of the fault. It has been applied successfully to differentiate air mass sensor faults from other process faults.

Keywords: Fault detection and diagnosis; Input and excitation design; Modeling, supervision and diagnosis of automotive systems; Automobile power trains; Automotive sensors and actuators; Automotive system identification and modeling; Parameter estimation and parity space based methods for FDI;

1. INTRODUCTION

Along with the rising complexity of many technical processes the requirements on modern diagnosis systems increase rapidly. Advanced methods of fault detection and fault diagnosis are needed in order to secure availability, reliability and safety of the supervised processes. These methods are supposed to detect also small faults early and to diagnose faults in the actuators, process components and sensors reliable. To satisfy the increasing requirements on the mentioned diagnosis systems, model-based methods of fault detection and fault diagnosis have been developed. A broad description of fault diagnosis systems is given in Isermann (2006).

2. MODEL-BASED FAULT DETECTION AND FAULT DIAGNOSIS METHODS

Model-based fault-detection methods use mathematical process models to relate data of several measurable variables. In recent years several approaches have been introduced, see e.g. Isermann (2006); Simani et al. (2003); Patton et al. (2000); Chen and Patton (1999); Gertler (1998) and especially with respect to engine applications e.g. Payri et al. (2006); Kimmich et al. (2005); Antory et al. (2004); Schwarte et al. (2003); Capriglione et al. (2003); Nyberg (2002). As shown in Fig. 1 the detection methods generate different features from measured input signals $\mathbf{U}$ and output signals $\mathbf{Y}$. The features, consisting of residuals $\mathbf{r}$, parameter estimates $\hat{\Theta}$ or state estimates $\hat{\mathbf{x}}$, are compared with nominal feature values. Thus feature changes can be detected and analytical symptoms $\mathbf{S}$ can be generated. These symptoms are analyzed using fault relevant process knowledge in order to determine the faults $\mathbf{F}$ and their associated properties Ξ like fault size and fault location.

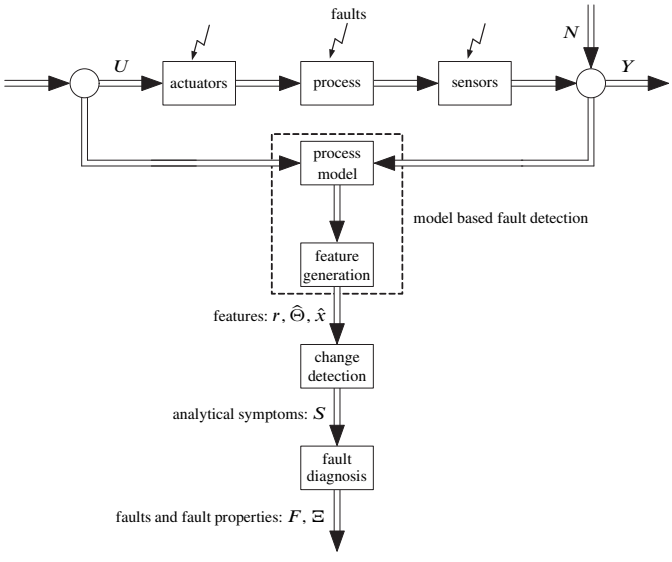

Fig. 1. Process model-based fault detection and diagnosis

Since those fault diagnosis systems use the measurable variables $\mathbf{U}$ and $\mathbf{Y}$ for feature generation and fault determination, they are limited by the available data and therefore by the actuator and sensor setup. For reasons of economy or technical feasibility the number of sensor data is generally restricted.

⋆ This work was supported by the Forschungsvereinigung Verbrennungskraftmaschinen e.V.

Additional information is achievable if the process can be excited with special test cycles. Such test cycles are generally used for fault-detection with parameter estimation methods, see, e.g., Isermann (2006). In the following a model-based fault-detection and localization method based on special input excitation is considered, which allows a deep insight into the process behavior.

3. FAULT DETECTION AND LOCALIZATION WITH SPECIAL INPUT EXCITATION

The underlying idea of the mentioned algorithm is to excite a multivariable system in such a way, that it is possible to detect and to locate faults by observing the effect of a certain input signal on the system's output.

3.1 Formal description of the observed systems

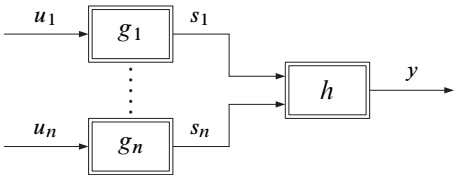

Fig. 2. Structure of the observed systems

The observed system (Fig. 2) is excited by the inputs

$$u_i : [0, \infty) \to \mathbb{R}, i = 1, \ldots, n \tag{1}$$

They affect the static nonlinear behavior of several actuators and processes. These are given by

$$g_i : \mathcal{C}(\mathbb{R}, \mathbb{R}) \to \mathcal{C}(\mathbb{R}, \mathbb{R}), g_i(u_i) := s_i, i = 1, \ldots, n \tag{2}$$

where $\mathcal{C}(A, B)$ is the space of all continuous functions from A to B. Thus the functionals g_i map the input signals u_i to the signals

$$s_i : \mathbb{R} \to \mathbb{R}, i = 1, \ldots, n \tag{3}$$

Furthermore the system consists of a common process and a sensor, which are given by

$$h : \mathcal{C}^n(\mathbb{R}, \mathbb{R}) \to \mathcal{C}(\mathbb{R}, \mathbb{R}), h(\mathbf{g}(\mathbf{u})) = h(\mathbf{s}) := y \tag{4}$$

The functional h maps all signals s_i to the output signal

$$y : \mathbb{R} \to \mathbb{R} \tag{5}$$

The bold letters in (4) indicate the tuples

$$\mathbf{u} = (u_1, \ldots, u_n), \mathbf{g} = (g_1, \ldots, g_n), \mathbf{s} = (s_1, \ldots, s_n) \tag{6}$$

3.2 Fault models

Any component fault may introduce changes in one of the parts g_i and h leading to the faulty output $\tilde{y}$. Component faults enclose any actuator and sensor fault as well as changes in the system's parameters and structure. These faults are described by the functional

$$f : \mathcal{C}(\mathbb{R}, \mathbb{R}) \to \mathcal{C}(\mathbb{R}, \mathbb{R}) \tag{7}$$

which affects either the common block h or one of the blocks g_i in the form

$$\tilde{h}(\mathbf{s}) = f(h(\mathbf{s})) \tag{8}$$

$$\tilde{g}_i(u_i) = f(g_i(u_i)), i = 1, \ldots, n \tag{9}$$

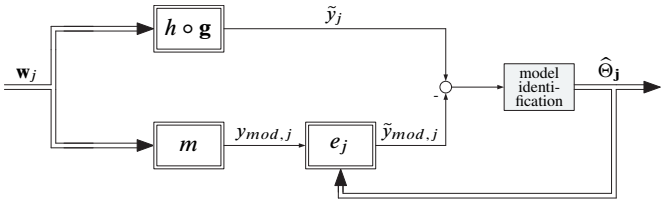

Fig. 3. Identification of the fault effect describing functions

3.3 Fault effect analysis

In order to observe the effect of a certain input signal on the system's output the procedure shown in Fig. 3 is used. The figure shows the excitation of the system $h \circ \mathbf{g}$ with an input signal $\mathbf{w}_j$. As will be explained in the next chapter the process is excited by n different signals labeled by the index $j, 1 \leq j \leq n$. The excitation with $\mathbf{w}_j$ results to the faulty output $\tilde{y}_j$. A process model m, which describes the system's nominal behavior, provides the output $y_{mod,j}$

$$m : \mathcal{C}^n(\mathbb{R}, \mathbb{R}) \to \mathcal{C}(\mathbb{R}, \mathbb{R}), m(\mathbf{w}_j) = y_{mod,j} \tag{10}$$

The output $y_{mod,j}$ is approximately equal to the corresponding process output in the fault free case

$$y_{mod,j} : \mathbb{R} \to \mathbb{R}, y_{mod,j} \approx h(\mathbf{g}(\mathbf{w}_j)) = y_j \tag{11}$$

The effect of the excitation on the faulty plant is measured by a functional e_j which maps the model output onto the faulty process output in the way

$$e_j : \mathcal{C}(\mathbb{R}, \mathbb{R}) \to \mathcal{C}(\mathbb{R}, \mathbb{R}), e_j(y_{mod,j}) = \tilde{y}_j \tag{12}$$

Their parameters $\hat{\Theta}_j$ are derived with use of an appropriate identification technique. In the following the functions e_j are referred to as fault effect describing functions FDFs.

3.4 Special input excitation

As stated above a suitable excitation needs to affect the faulty part in such a way, that it is possible to detect and to locate it by observing the FDFs. For this purpose n input signals $\mathbf{w}_j$ are used here. Each excitation signal affects only the input u_j, whereas the other $n - 1$ inputs u_k are left at a constant level c_k. Thus the input signal $\mathbf{w}_j$ is of the form $\mathbf{w}_j = (c_1, \ldots, c_{j-1}, u_j, c_{j+1}, \ldots, c_n)$. Since the inputs $u_k, k \neq j$ are not excited the corresponding outputs s_k have a constant value γ_k.

3.5 Fault detection and localization

Using the input signals $\mathbf{w}_j$ the effect on the n corresponding FDFs depends on the location of the fault and the excited input u_j.

Fault affecting h First the effects of faults in the common part on the FDFs shall be analyzed. Such faults affect block h as stated in (8). Combining (8) and (12) and using (11) the n FDFs e_j are found to

$$\begin{aligned} e_j(y_{mod,j}) &\overset{(12)}{=} \tilde{y}_j = \tilde{h}_j(\mathbf{g}(\mathbf{w}_j)) \\ &\overset{(8)}{=} f(h(\mathbf{g}(\mathbf{w}_j))) = f(y_j) \overset{(11)}{\approx} f(y_{mod,j}) \end{aligned} \tag{13}$$

Thus the n FDFs are equal to the functional f.

Fault affecting the block g_l Now faults of the type as given by (9) are discussed. It is assumed, that such faults affects only

one block g_l. For these faults the n FDFs e_j are found to (using (9) and (12))

$$e_j(y_{mod,j}) \overset{(12)}{=} \tilde{y}_j \overset{(9)}{=} h(s_1, \ldots, f(s_l), \ldots, s_n) \quad (14)$$

If the input u_l is excited (14) can be written as

$$e_l(y_{mod,l}) = \tilde{y}_l = h(\gamma_1, \ldots, f(s_l), \ldots, \gamma_n) \quad (15)$$

Thus the FDF e_l depends on the fault and the structure of h. If any other input u_j, $j \neq l$ is excited (14) can be written as

$$\begin{aligned} e_j(y_{mod,j}) =& \tilde{y}_j \\ =& h(\gamma_1, \ldots, s_j, f(s_l), \ldots, \gamma_n) \\ =& h(\gamma_1, \ldots, s_j, \gamma_l + \delta_l, \ldots, \gamma_n), \delta_l \in \mathbb{R} \end{aligned} \quad (16)$$

These $n-1$ FDFs depend only on the structure of h. Since the fault in g_l is not excited it returns an offset δ_l on γ_l. Thus it is possible to determine the $n-1$ FDFs e_j, $j \neq l$ with knowledge of h.

Conclusion In practice the FDFs e_j will differ from each other if a fault in block g_l occurs. This difference can be used to locate the fault since 1. for faults in h all FDFs are equal and 2. for faults in g_l at least one FDF will differ from the others. Thus the FDFs need to be compared in order to decide where the fault occurred. How this comparison can be achieved depends mainly on the underlying process as will be shown in the case study in section 4.

3.6 Classification of the algorithm

The fault detection algorithm could be classified as a variant of parity equations, because models which describe the fault free case are paralleled to the supervised process. Unlike the parity equation approach the process and model output are not compared by residuals.

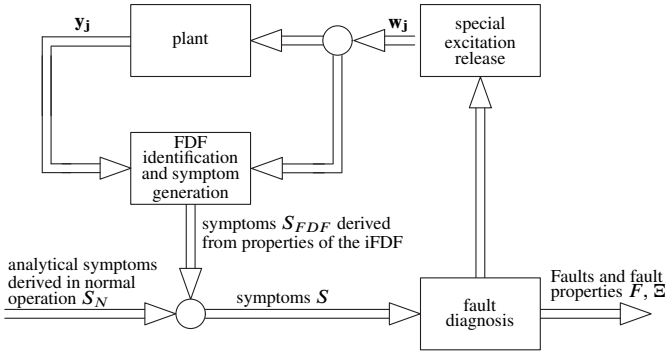

Fig. 4. Flowchart: Fault diagnosis, active excitation and fault describing functions

A significant difference to other fault detection and diagnosis methods is the algorithm inherent overlap of both tasks. The fault detection procedure ends with comparing the FDFs and together with the detection of a fault its location is derived.

Nevertheless in many practical applications the method will be used to derive extra information of already detected faults, because the described excitation will be inapplicable in normal operation of the supervised plant. Thus the excitation will be released only, if a detailed fault diagnosis cannot be derived with the given information.

The approach could therefore be classified as a fault location method within the fault diagnosis task, which releases the active excitation and uses the additional symptoms S_{FDF} to obtain more detailed information of the faults F and their properties Ξ (see Fig. 4).

4. APPLICATION TO A DIESEL ENGINE FOR HFM SENSOR FAULT-DETECTION AND ISOLATION

The following case study deals with the application of the above mentioned algorithm to the intake air system of a modern Diesel engine.

4.1 Experimental setup

All experiments were performed on a 1.9l Opel common rail Diesel engine, which is equipped with exhaust gas recirculation and exhaust gas turbo charger with variable turbine geometry. During the experiments the engine was run in idle. The idle state provides suitable operation conditions for an excitation release and can be driven in a garage. This is important because during the excitation no additional driver input is allowed. Thus the test is best been executed by servicing staff.

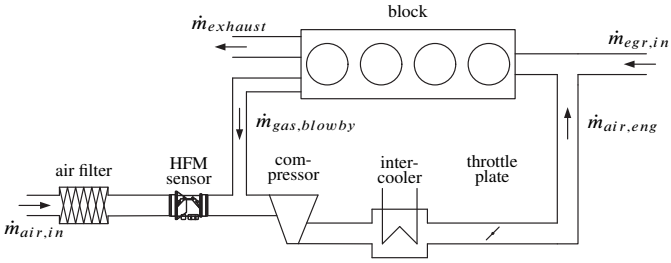

Fig. 5. Intake system

Fig. 5 shows a schematic diagram of the intake air system. Intake air pours in the system and is filtered first. Then a HFM sensor measures the air mass flow $\dot{m}_{air,in}$. Next, blow-by $\dot{m}_{gas,blowby}$ enters the tube between HFM sensor and compressor. Blow-by is the small amount of unburned fuel and exhaust gases which leak around the piston rings and enter the crankcase. Next, the mixture $\dot{m}_{air,eng}$ of fresh air and blow-by is compressed and cooled down. After that $\dot{m}_{air,eng}$ passes the throttle and enters the cylinders along with the recirculated exhaust gas $\dot{m}_{egr,in}$. Inside the cylinders fuel is injected and combustion takes place. Finally, the exhaust gas $\dot{m}_{exhaust}$ as well as the blow-by leaves the block.

4.2 Considered faults

Soiling of the HFM sensor The first considered fault is a HFM sensor fault. A faulty sensor is often caused by soiling. In order to analyze the effect of soiling on the sensor's output a deeper insight into the principles of the air mess meter is necessary.

The working principle of the applied thermal mass flow sensor HFM5 (see Bauer (2004)) is called calorimetric (for a detailed description see Nguyen (1999)). These sensors measure the displacement of the temperature profile around a heating element caused by the air flow, as shown in Fig. 6. First, the air mass flow passes the upstream thermistor which measures the air's temperature. Next, the air mass is warmed up by a temperature controlled heater. The resulting air temperature depends on the flow velocity: The slower the air passes the heater, the warmer it gets. By measuring the air's temperature in the downstream thermistor again, one gets a measure of the flow velocity. It is

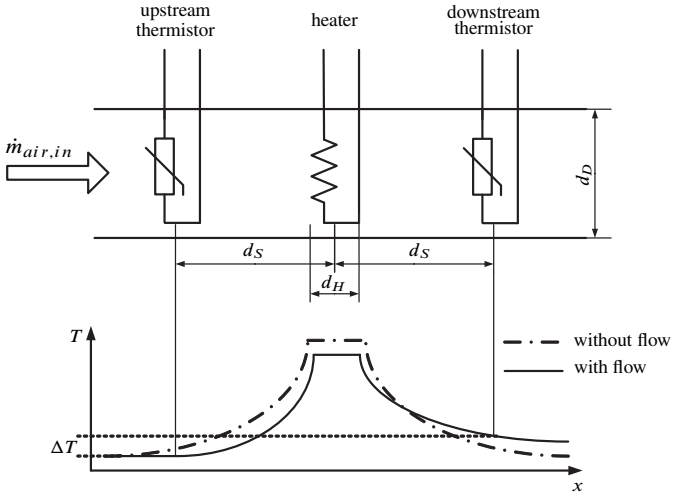

Fig. 6. Principle HFM sensor functionality

proportional to the temperature difference of the downstream and the upstream thermistor. Thus the output of the sensor respectively the temperature difference ΔT depends on the air flow $\dot{m}_{air,in}$ and the heater power P. The analytical model introduced in Nguyen (1999) determines ΔT with ρ as the air density, c as its heat capacity, v as its average velocity, λ as its thermal conductivity, the dimensions d_S, d_H and d_D as depicted in Fig. 6. Given a cylindric flow channel, the model is found to

$$\Delta T(v,P) = T_0 \cdot \left(e^{\gamma_2\left(\frac{d_S-d_H}{2}\right)} - e^{\gamma_1\left(\frac{-d_S+d_H}{2}\right)} \right) =: T_0 \cdot q_1(v) \tag{17}$$

$$T_0(v,P) = \frac{P}{2\cdot\lambda\cdot d_H + \pi\cdot d_D^2\cdot\lambda\,(\gamma_1-\gamma_2)} =: \frac{P}{q_2(v)} \tag{18}$$

$$\gamma_{1,2} = \frac{v \pm \sqrt{v^2 + \frac{2a^2}{d_D^2}}}{2a}, \text{ with } a = \frac{\lambda}{\rho c} \tag{19}$$

Soiling may affect the heater as well as the thermistors. In both cases the measured and the effective air mass flow will differ.

Fallen off blow-by tube The second fault is a fallen off blow-by tube. The effect of this fault on the air system in general and the HFM sensor in particular differs. During normal operation the engine vacuum is from the intake manifold, through the blow-by tube, through various filters and to the crankcase. Ambient air enters the intake manifold through the air filter and HFM sensor. If the blow-by tube falls off this air mass flow splits into a mass flow through the sensor and one through the arisen leak. In sum the new mass flow to the engine may differ a little from the normal one, because less power is needed to generate the engine vacuum. Since this difference is marginal, it is assumed that the mass flow into the engine keeps constant. Thus there is no effect of the fault on the air system in general. However there is a effect on the HFM sensor in particular, because the mass flow through the sensor is at a significant lower level.

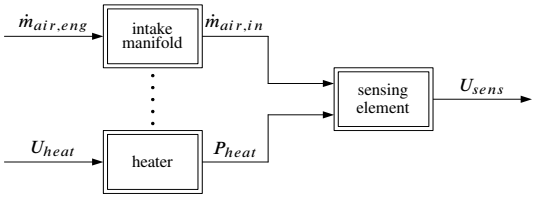

Fig. 7. System structure. The use of the heater power U_{heat} and the air mass flow $\dot{m}_{air,eng}$ as inputs leads to a suitable system structure (see section 3.1).

4.3 Input selection and sensor modification

Both faults may lead to a lower sensor output voltage, but do not have an effect on the rest of the engine. In order to differentiate these faults using the above mentioned algorithm, suitable inputs need to be found. In terms of section 3 inputs are suitable, if their use leads to a system structure, in which the sensor and the intake manifold are not part of the same block. It is obvious to investigate the use of the various actuators like turbo charger, throttle plate, egr valve or the engine speed as inputs, first. Their use excites the air mass flow through the engine $\dot{m}_{air,eng}$ and thus the mass flows through the leakage as well as through the sensor. This means that the use of several of the mentioned actuators is not suitable, because both, the intake manifold and the HFM sensor, would be part of the common block h.

Equations (17) to (19) show that the output voltage U_{sens} of the sensor depends on the velocity of the air mass flow through the sensor $m_{air,in}$ and the heater's temperature T_{heat}. These variables can be excited by the heater power P_{heat} or rather its supply voltage U_{heat} and the air mass flow $\dot{m}_{air,eng}$. This leads to the system structure shown in Fig. 7. Thus using these inputs the intake manifold, the heater and the sensing elements are part of different blocks, as it is needed for differing the above mentioned faults.

The air mass flow can be differed by several actuators e.g. the throttle plate. The heater temperature is normally controlled by an electronic circuit within a supply voltage range from 8V to 17V at terminal 2 as shown in Fig. 8 below the line. Beyond the 8V threshold the temperature can not reach the desired value so that the maximum possible voltage is applied to the heater. Thus this area can be used for differing its power. For this purpose the sensor has been simply modified with a common selector circuit in order to control the supply voltage U_{heat} by a Dspace rapid prototyping system as shown in Fig. 8 above the line. Since the heater power depends on it's supply voltage as well as on the air flow velocity, the input power is controlled digitally in closed-loop.

4.4 Fault specific characteristics of the fault effect describing functions

With the aforesaid the process in steady state, according to Fig. 2 and Fig. 7 respectively, is given by (see (17) to (19))

$$u_1 = \dot{m}_{air,eng} \tag{20}$$

$$u_2 = U_{heat} \tag{21}$$

$$y = U_{sens} = s(\Delta T) \tag{22}$$

$$= s\left(P_{heat}(U_{heat}) \cdot \frac{q_1(v_{air,in})}{q_2(v_{air,in})} \right) \tag{23}$$

$$=: s\left(P_{U_{heat}} \cdot q_{v_{air,in}} \right) \tag{24}$$

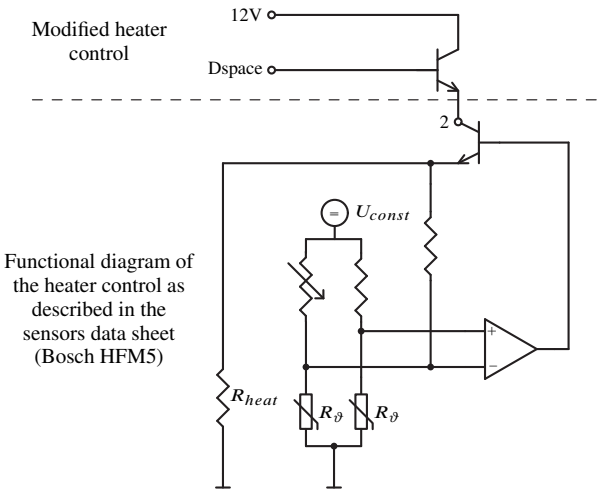

Fig. 8. Functional diagram of the modified sensor heater

The functional s describes the sensing element of the air mass meter which measures the temperature difference. Since the temperature dependence of the resistances is nearly linear in the studied working points, s is assumed as a linear function of ΔT with the slope a:

$$s(\Delta T) = a \cdot \Delta T = a \cdot P_{U_{heat}} \cdot q_{v_{air,in}} \tag{25}$$

Because faults in each block g_1 (intake manifold), g_2 (heater) and h (sensing element) need to be separated, information about fault effects and the structure of h have to be taken into account as described in section 3.5.

Faulty heater First, the excitation of $\dot{m}_{air,eng}$ is analyzed. The faulty output $\tilde{y}_{\dot{m}_{air,eng}}$ is found to

$$\tilde{y}_{\dot{m}_{air,eng}} \overset{(16),(25)}{=} a \cdot (\gamma_{P_{U_{heat}}} + \delta_{P_{U_{heat}}}) \cdot q_{v_{air,in}} \tag{26}$$

Since s is linear and the heater power is at a constant lower or higher level $\gamma_{P_{U_{heat}}} + \delta_{P_{U_{heat}}}$ the corresponding FDF $e_{\dot{m}_{air,eng}}$ can be approximated by a linear function with the slope α:

$$e_{\dot{m}_{air,eng}}(y_{mod,\dot{m}_{air,eng}}) = \alpha \cdot y_{mod,\dot{m}_{air,eng}} \tag{27}$$

$$\overset{(11),(25)}{=} \alpha \cdot a \cdot \gamma_{P_{U_{heat}}} \cdot q_{v_{air,in}} \tag{28}$$

$$\overset{(12),(26)}{=} (a \cdot \gamma_{P_{U_{heat}}} + a \cdot \delta_{P_{U_{heat}}}) \cdot q_{v_{air,in}} \tag{29}$$

$$\Longleftrightarrow \alpha = 1 + \frac{\delta_{P_{U_{heat}}}}{\gamma_{P_{U_{heat}}}} \tag{30}$$

Next, the excitation of the heater supply voltage U_{heat} and the associated FDF $e_{U_{heat}}$ is investigated. The excitation of U_{heat} leads to the faulty output

$$\tilde{y}_{U_{heat}} \overset{(15),(25)}{=} a \cdot f(P_{U_{heat}}) \cdot \gamma_{q_{v_{air,in}}} \tag{31}$$

As described in (15) nothing can be stated on $e_{U_{heat}}$, without further information on the fault f.

Fallen off blow-by tube If the air mass flow $\dot{m}_{air,eng}$ is excited, the faulty output $\tilde{y}_{\dot{m}_{air,eng}}$ is given by

$$\tilde{y}_{\dot{m}_{air,eng}} \overset{(15),(25)}{=} a \cdot \gamma_{P_{U_{heat}}} \cdot f(q_{v_{air,in}}) \tag{32}$$

Since the temperature difference (see (17) to (19)) depends nonlinear on the the flow velocity $v_{air,in}$, the FDF $e_{\dot{m}_{air,eng}}$ can not be approximated by a linear function in practice. However, without further knowledge on f nothing else can be stated (see (15)).

The excitation of U_{heat} leads to the faulty output

$$\tilde{y}_{U_{heat}} \overset{(16),(25)}{=} a \cdot P_{U_{heat}} \cdot (\gamma_{q_{v_{air,in}}} + \delta_{q_{v_{air,in}}}) \tag{33}$$

Again (see section 4.4.1 and (27) to (30)), the FDF $e_{U_{heat}}$ can be approximated by a linear function with the slope α:

$$e_{U_{heat}}(y_{mod,U_{heat}}) = \alpha \cdot y_{mod,U_{heat}} \tag{34}$$

$$= \left(1 + \frac{\delta_{q_{v_{air,in}}}}{\gamma_{q_{v_{air,in}}}}\right) \cdot y_{mod,U_{heat}} \tag{35}$$

Conclusions Because faults in the sensing elements lead to excitation independent FDFs F_h (see (13)) faults in the air mass meter and the fallen off blow-by tube can be differed as Table 1 shows. Note that soiling of the sensor often affects the heater as well as the sensing element. This fault is nevertheless isolable of the fallen off blow-by tube, because the combination of a nonlinear FDF, if $\dot{m}_{air,eng}$ is excited, and a linear one, if U_{heat} is excited, keeps unique. Thus it is of main interest whether

Table 1. Faults and corresponding FDF properties

	excitation of	
	$\dot{m}_{air,eng}$	U_{heat}
faulty heater	linear FDF	nothing can be stated
faulty sensing element	F_h	F_h
fallen off blow-by tube	nonlinear FDF	linear FDF

a FDF is linear or nonlinear. An easy way to check this is to use a linear model for the identified fault effect describing functions (iFDFs) $\hat{e}_{lin,j}$ which fits $\tilde{y}_j$ in a least square sense. An appropriate residual is given by

$$r_{nonlin,j} = \tilde{y}_j - \hat{e}_{lin,j}(y_{mod,j}). \tag{36}$$

This residual is approximately zero if the underlying FDF is a linear function and nonzero otherwise.

4.5 Experimental results

The inputs were excited as shown in Fig. 9. The air mass flow was excited by differing the throttle plate position s_{tp}. Because the static behavior of the system is of interest the excitation signals must not excite the system's dynamics. In order to reduce the attended measurement time and to enhance the number of measured data, quasi-stationary input signals (see Ward et al. (2002); Leithgöb et al. (2005)) are used. Two models were identified using the LOLIMOT algorithm (see Nelles (2001)) with a maximum of five local linear models. The considered faults were implemented by

(1) reducing the desired heater supply voltage by 5% (Fig. 11),
(2) reducing the output voltage by 5% (Fig. 12) and
(3) removing the blow-by tube (Fig. 13).

As shown in Fig. 10 to 13 only the removed blow-by tube causes a nonlinear FDF and is isolable from a sensor fault.

5. CONCLUSION

First the use of special excitation and fault describing functions for fault isolation was developed. Next, it was shown that the use of the described method on the intake air system of a

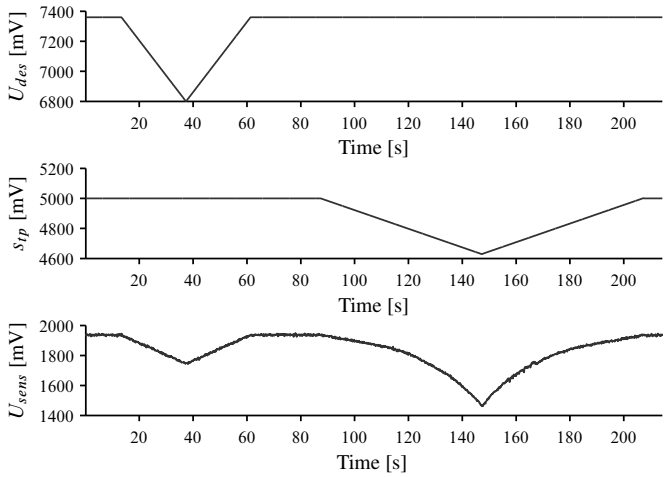

Fig. 9. Excitation of the heater power by U_{des} and the air mass flow by s_{tp} as well as the appropriate sensor output voltage U_{sens} in the fault free case

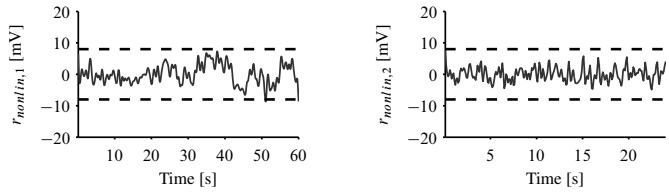

Fig. 10. $r_{nonlin,j}$ in the fault free case

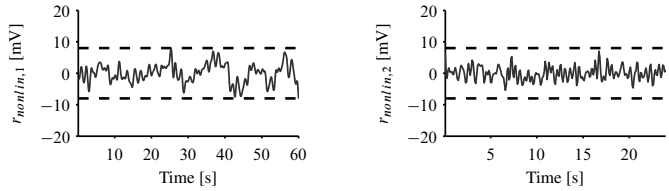

Fig. 11. $r_{nonlin,j}$ when the desired heater supply voltage has been reduced

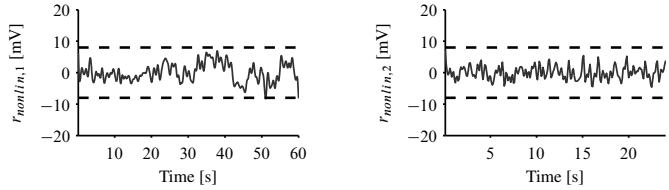

Fig. 12. $r_{nonlin,j}$ if the output voltage is reduced

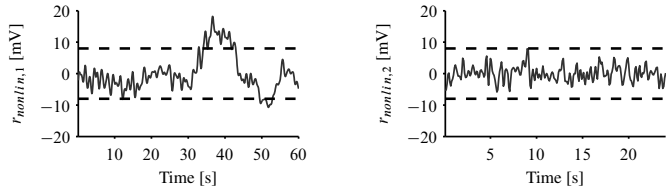

Fig. 13. $r_{nonlin,j}$ when the blow-by tube has been removed

modern Diesel engine allows the differentiation of a negative HFM sensor fault and a fallen off blow-by tube. Summing up, the provided method is a suitable instrument for fault isolation in multivariable systems.

In further studies the method will be applied to additional systems and future research will focus on the use of fault describing functions in dynamic systems as well as systems with feedback.

REFERENCES

D. Antory, U. Kruger, G. Irwin, and G. McCullough. Fault diagnosis in internal combustion engines using non-linear multivariate statistics. *Proceedings of the Institution of Mechanical Engineers, Part I: Journal of Systems and Control Engineering*, 219(4):243–258, 2004. doi: 10.1243/095965105X9614.

Domenico Capriglione, Consolatina Liguori, Cesare Pianese, and Antonio Pietrosanto. On-line sensor fault detection, isolation, and accommodation in automotive engines. *IEEE Transactions on Instrumentation and Measurement*, 52(4): 1182–1189, August 2003. doi: 10.1109/TIM.2003.815994.

Jie Chen and Ron J. Patton. *Robust model-based fault diagnosis for dynamic systems*. Kluwer, 1999.

Janos J. Gertler. *Fault detection and diagnosis in engineering systems*. Marcel Dekker, New York, 1998.

Horst Bauer (Robert Bosch GmbH), editor. *Automotive electrics, automotive electronics*. Vieweg, 2004.

Rolf Isermann. *Fault-diagnosis systems*. Springer, 2006.

Frank Kimmich, Anselm Schwarte, and Rolf Isermann. Fault detection for modern diesel engines using signal- and process model-based methods. *Control Engineering Practice*, 13: 189–203, 2005.

R. Leithgöb, M. Bollig, M. Büchel, and F. Henzinger. Methodology for efficient calibration of model based ecu structures. In *1. Internationales Symposium für Entwicklungsmethodik*, 2005.

Oliver Nelles. *Nonlinear system identification*. Springer, 2001.

Nam-Trung Nguyen. Thermal mass flow sensors. In John G. Webster, editor, *The Meauserment, Instrumentation, and Sensors Handbook*, pages 100–119. CRC Press, 1999.

Mattias Nyberg. Model-based diagnosis of an automotive engine using several types of fault models. *IEEE Transactions on Control Systems Technology*, 10(5):679–689, September 2002. doi: 10.1109/TCST.2002.801873.

Ron J. Patton, Paul M. Frank, and Robert N. Clark. *Issues of fault diagnosis for dynamic systems*. Springer, 2000.

F. Payri, J. M. Luján, C. Guardiola, and G. Rizzoni. Injection diagnosis through common-rail pressure measurement. *Proceedings of the Institution of Mechanical Engineers, Part D: Journal of Automobile Engineering*, 220(3):347–357, 2006. doi: 10.1243/09544070JAUTO34.

Anselm Schwarte, Frank Kimmich, and Rolf Isermann. Model-based fault detection of a diesel engine with turbo charger - a case study. In *5th IFAC Symposium on Fault Detection, Supervision and Safety of Technical Processes (SAFEPROCESS)*, Washington, D.C., USA, June 2003.

Silvio Simani, Cesare Fantuzzi, and Ron J. Patton. *Model-based fault diagnosis in dynamic systems using identification techniques*. Springer, 2003.

Matthew Ward, Chris Brace, Thom Hale, and Robert Ceen. Investigation of 'sweep' mapping approach on engine testbed. In *SAE 2002 World Congress & Exhibition Technical Papers*, 2002.